ACI STRUCTURAL JOURNAL TECHNICAL PAPER

Title no. 106-S03

Moment-Curvature and Strain Energy of Beams with External Fiber-Reinforced Polymer Reinforcement

by Paththini M. M. Achintha and Chris J. Burgoyne

To calculate the load at which fiber-reinforced polymer (FRP) plates will debond from a reinforced concrete (RC) beam using fracture mechanics principles based on energy release rates, it is necessary to accurately determine the strain energy in the beam. This study presents a moment-curvature model for an RC beam with the presence of a net axial force that is due to the force in the FRP plate. The classical Branson analysis only covers the case of a cracked-elastic concrete beam with no axial force. The paper shows how the model can be extended into the inelastic regime and can be used to determine the moment-curvature relations on loading. Comparisons with the available test data have shown good correlation. The model is then extended into an unloading regime for the strain energy determinations of RC beams with external reinforcement, which may be bonded or partially debonded.

Keywords: Branson's model; elastic stiffness; moment-curvature; strain energy.

INTRODUCTION

Reinforced concrete (RC) beams flexurally strengthened with externally-bonded fiber-reinforced polymer (FRP) plates often fail by plate debonding, but a rational analytical approach to these failures has yet to be developed. Due to the typically premature and brittle nature of these debonding failures, inadequately designed strengthening applications may become ineffective and reduce the level of safety. A proper understanding of the concrete-FRP interface debonding is required for safe and reliable applications of externally bonded FRP systems for strengthening of RC elements.

The debonding mechanisms of plates glued to concrete structures are proving very difficult to analyze. The temptation is to model the interface using finite elements, but this procedure is doomed to failure. A reentrant corner leads to an infinite stress concentration, so the values returned by a finite element program are governed by the smallness of the elements used. The sort of model that can be used to follow the crack tip behavior in fracture mechanics studies requires far more detail than will ever be available to the designer or analyst of an RC beam, who would be forced to make unwarranted assumptions about interface properties. There are doubts about whether linear models are accurate for concrete applications.

Fracture-mechanics models, such as Hutchinson and Suo's[1] interface fracture model for layered elastic materials, offer a better alternative for interface debonding problems. They assume that, because flaws are inevitable in the interface, what matters is whether these flaws can propagate. When an existing flaw extends, the energy needed to form associated new surfaces depends on the interface fracture energy and must be compared with the energy released by the system, which in turn depends on the change of stored strain energy. This paper is concerned only with the determination of that strain energy as an essential prerequisite to a debonding analysis that is described elsewhere.[2]

It is not a trivial problem to determine the strain energy stored in an RC beam, to which is attached an FRP plate that may be debonded over part of its length. This is particularly important in a fracture mechanics analysis because decisions about whether a flaw can propagate, and hence whether the structure is safe, depend on the (potentially small) difference in strain energy between the states before and after propagation.

This study relates to an analysis of the strain energy state of a beam with a partially bonded FRP plate. It does not attempt to explain how the beam got into the present state, nor the load at which the debonded region will extend, which may well be associated with failure. Those processes are discussed in an associated paper.[2] This paper concentrates on the analysis at one debonded state only and is aimed at determining the strain energy in the current state, which is the essential parameter needed for the wider analysis.

When an RC beam cracks, its stiffness does not immediately change to that of a section where the tension-concrete can be fully disregarded. Various empirical models, such as Branson's I_{eff} concept,[3] have been used to model this behavior, primarily with a view to being able to predict the deflections of RC beams to check their compliance with code limits. Such models normally work in moment-curvature (M-κ) space rather than stress-strain (σ-ε) space and thus do not attempt to model individual cracks. Two versions are normally presented: one designed to model the overall beam stiffness and the other to determine the local curvature.

An external FRP plate will act as a prestressing element, inducing both force and moment in the original RC beam (Fig. 1); most existing models do not cope with this effect. It is not possible to consider the FRP as a second layer of reinforcement because it is necessary to consider the strain state when the FRP is partly debonded. The mechanics of stress transfer from concrete to FRP are different from that of reinforcing bar and most of the existing models (such as those of Faruqi et al.[4] and El-Mihilmy and Tedesco[5]) are not calibrated for two different levels (or types) of reinforcement. The new model is first explained and then verified by comparisons with the available test data.

The strain energy in a beam at a given state can be calculated as the energy that is recoverable upon complete unloading. It will thus be necessary to determine the M-κ relationship on loading, from which the stress and deflection state of the beam can be found, and then the corresponding M-κ relations for unloading, from which the amount of stored energy can be determined.

ACI Structural Journal, V. 106, No. 1, January-February 2009.
MS No. S-2006-494.R3 received March 18, 2008, and reviewed under Institute publication policies. Pertinent discussion including author's closure, if any, will be published in the November-December 2009 *ACI Structural Journal* if the discussion is received by July 1, 2009.

Paththini M. M. Achintha *is a PhD Candidate at the University of Cambridge, Cambridge, UK. He received his BScEng in 2003 from the University of Moratuwa, Moratuwa, Sri Lanka. His research interests include the application of fiber-reinforced polymers in civil engineering and fracture mechanics of concrete.*

Chris J. Burgoyne *is a Reader in Concrete Structures at the University of Cambridge. He is a member of ACI Committee 440, Fiber Reinforced Polymer Reinforcement. His research interests include advanced composites applied to concrete structures.*

RESEARCH SIGNIFICANCE

The analysis presented herein provides an essential tool that will enable fracture mechanics to be used to determine the load at which FRP plates will debond from RC beams. This will obviate the need for finite element analyses to be used in situations where there is an infinite stress concentration and where the exact details of the interface geometry and properties are unknowable.

TENSION STIFFENING

Calculations of the stiffness of RC beams at the working load must make some allowance for the additional stiffness caused by the tensile stresses in the concrete that is partially cracked. A detailed analysis would require knowledge of the exact location of the reinforcement and each of the cracks; such information is effectively unknowable. For most practical purposes, it has been sufficient to determine the effective stiffness of the section or the beam using an interpolation formula. That derived by Branson[3] is most commonly used, and that model is extended herein.

Tension stiffening models, such as Branson's, have limitations. They only apply to RC beams subject to pure bending, which can be regarded as a simple couple, so there is no need to define a particular reference axis and no need to worry about the distinction between the centroid and the neutral axis. In the present study, that will no longer be true because the RC beam has to be analyzed under the moment and axial force induced by the external FRP plate (Fig. 1), as well as the external load.

These methods are primarily concerned with stiffness and not normally used to determine the stresses in the beam that are assumed to be adequate because separate checks (either permissible stress or section strength) would be performed in association. The present method, however, requires the satisfaction of a compatibility condition between the FRP and the concrete, which means that strong assumptions need to be made about the strains, and hence stresses, in the cross section; and these will have to be determined from the effective stiffness.

Tension stiffening models were originally developed for situations where the beam was at the working load, so the stresses everywhere would be relatively low and the material could be assumed to be linearly elastic. Herein the model is to be applied to sections that are being strengthened to carry loads that would have caused the original section to fail, so at least some of the steel in the section may be yielding and the concrete stresses will be high enough that nonlinearity should be taken into account. That will be done by determining an equivalent elastic stiffness.

The model described in this paper will subsequently be used to answer the question "Will this interface crack extend?" (which presupposes that a preexisting crack must be present.) It is not concerned with how that crack or flaw forms in the first place. The case of an FRP plate debonding from its end is relatively simple because the peeled part of the plate can effectively be ignored. But if the plate debonds from somewhere in the middle of the beam, there will be two

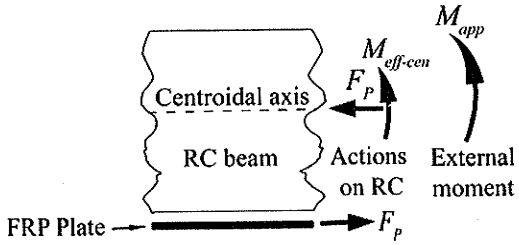

Fig. 1—Actions of longitudinal section.

end regions, both fully bonded, separated by a region in which the FRP plate is debonded but constrained by a compatibility condition.

As a final complication, all the analysis described previously assumes knowledge of the force in the FRP plate, but this is not known from the beginning and must be found iteratively.

Thus, the objective is to find a method that can determine the M-κ behavior of a partially cracked beam when being loaded and then unloaded, subject to an applied moment and an axial force, which must satisfy compatibility conditions with the external reinforcement that may be bonded or locally unbonded, using materials that may be nonlinear—all of which must sit within a nonlinear loop in which the force in the FRP plate is unknown.

BRANSON'S I_{eff} EXPRESSION

Branson[3] derived an expression (Eq. (1)) for the effective second moment of area (I_{eff}) that indirectly accounts for tension stiffening effects of cracked concrete and successfully predicts M-κ relations of RC beams. The stiffness of a cracked RC beam section is interpolated between the uncracked state (I_{un}), where the concrete is fully effective in tension, and the fully cracked state (I_{fc}), where there is no tension stiffening. An interpolation coefficient K represents the extent-of-cracking of the section

$$I_{eff} = KI_{un} + (1 - K)I_{fc} \quad (0 \le K \le 1) \tag{1}$$

$$K = \left(\frac{M_{cr}}{M_{app}}\right)^4 \tag{2}$$

where M_{cr} and M_{app} are the moments causing first cracking and the externally applied moment, respectively, and I_{eff} is taken as I_{un} when $M_{app} \le M_{cr}$. (When it is only necessary to find the average I_{eff} of the entire beam, for example to calculate the midspan deflection, the exponent in Eq. (2) is reduced from 4 to 3.[6])

The variable I_{eff} in Eq. (1) is the effective second moment of area of the equivalent transformed concrete section of modulus E_c, so curvature of the section (κ) can be determined from

$$\kappa = \frac{M_{app}}{E_c I_{eff}} \tag{3}$$

As an alternative, Eurocode 2[7] suggests interpolating the curvature of a partially cracked section between the corresponding uncracked and fully cracked curvatures, based on stress in the tension steel at the given applied moment (M_{app}) and the moment causing the first cracking (M_{cr}). Both values are calculated assuming a fully-cracked section. In addition, account is taken of bond with the steel and the type of

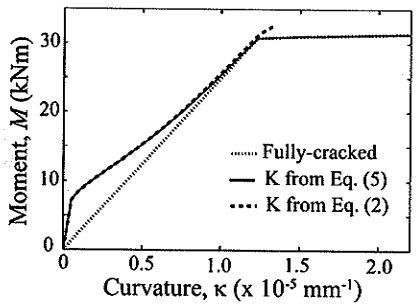

Fig. 2—M-κ comparison of present model with Branson's original. (Note: 1 kNm = 0.737 ft-kips; 10^{-5} mm^{-1} = 2.54 × 10^{-4} $in.^{-1}$.)

loading, but there is insufficient experimental evidence in the literature to back up the model. Local curvature determinations using Branson's concepts (Eq. (1) to (3)) have been widely verified for conventional RC beams; they will now be extended to deal with the more complex problem of beams with external FRP plates.

PROPOSED MOMENT-CURVATURE MODEL

Branson's method will need modifying to take account of several factors. The overall objective is to determine the equivalent elastic stiffness (EI_{eq}) of the RC portion of a partially cracked strengthened section, by interpolating between those from the uncracked and fully cracked section analyses, using materials that may be nonlinear.

Actions on a strengthened section

In a strengthened section, the FRP plate can be considered as a prestressing element, inducing both force and moment on the original RC section, even when fully bonded (Fig. 1). The RC section is analyzed under the action of a compressive force F_p (the force in the FRP plate) and an effective moment ($M_{eff\text{-}cen}$), both acting at the RC section's centroid. The variable $M_{eff\text{-}cen}$ is related to the externally applied moment (M_{app}) by Eq. (4). The values h, t_a, and t_p in Eq. (4) are the depth of the RC section, and the thicknesses of the adhesive layer and the FRP plate, respectively. The value α is the centroidal axis depth of the section, the location of which will be discussed in the following

$$M_{eff\text{-}cen} = M_{app} - F_p \times (h + t_a + t_p/2 - \alpha) \quad (4)$$

The value F_p is not yet known but can be determined by satisfying the relevant compatibility condition. In a bonded section, strain compatibility is satisfied locally; but if unbonded, there only needs to be compatibility of extension between the FRP plate and the bottom of the concrete beam over the unbonded region.

A modified interpolation coefficient

When the amount of cracking of an RC section increases, the tension stiffening eventually becomes ineffective. In Branson's model, the stiffness becomes asymptotic to the fully cracked state but never reaches it. That model was intended to represent sections at the working load and well below yield of the reinforcement. The present model will apply to beams where the loads cause yield of the conventional reinforcement and rely on the FRP for security. It can be expected that the fully cracked state will be reached because that is why the beam needed strengthening in the first place.

It will be assumed that the section is fully cracked at the moment causing first yielding of tension steel (M_y) and a slightly modified form of the interpolation factor used in Eq. (1) is proposed

$$K = \left(\frac{M_{cr}}{M_{app}}\right)^4 \left\{1 - \left(\frac{M_{app} - M_{cr}}{M_y - M_{cr}}\right)^4\right\} \quad (5)$$

This expression has the property that K is zero when $M_{app} = M_y$. When the M_y:M_{cr} ratio is greater than approximately 3, which would be the case for most practical RC beams, the difference between the predictions of Eq. (2) and (5) is negligible (as shown in Fig. 2) and avoids a discontinuity in the stiffness when the section yields.

Equation (5) allows the extent of cracking of a partially cracked section at any given M_{app} to be represented as a function of M_{cr}, M_y, and M_{app}. Only a part of the corresponding externally applied moment is effective on the RC section (Fig. 1 and Eq. (4)) and hence the relevant effective moments should be compared; these depend on the choice of the reference axis. To avoid unrealistic contributions due to varying eccentricities of the force in the FRP, a fixed reference axis will be used for the comparison; the middepth axis of the beam is chosen and the corresponding effective moments are denoted as $M_{cr\text{-}mid}$, $M_{y\text{-}mid}$, and $M_{app\text{-}mid}$, respectively. Thus, the interpolation coefficient used in the present model becomes

$$K_p = \left(\frac{M_{cr\text{-}mid}}{M_{app\text{-}mid}}\right)^4 \left\{1 - \left(\frac{M_{app\text{-}mid} - M_{cr\text{-}mid}}{M_{y\text{-}mid} - M_{cr\text{-}mid}}\right)^4\right\} \quad (6)$$

Equivalent elastic stiffnesses for inelastic sections

In normal RC design with under-reinforced sections, once the steel has yielded there is little point in determining the curvature because the section is on the point of failure. But with a strengthened beam, the section may have a considerable reserve of capacity after steel yield, so it is important to be able to determine the strain energy in such sections. At high strains, the concrete is nonlinear and steel will yield, so a cracked-elastic analysis is not applicable. It is possible, however, to define the equivalent elastic stiffness (EI_{eq}) of a strengthened section to use in place of the elastic stiffness (the product of E_c and I_{eff}) used by Branson

$$EI_{eq} = \frac{M_{eff\text{-}cen}}{\kappa} \quad (7)$$

where κ and $M_{eff\text{-}cen}$ are the curvature and the effective moment on the RC section about its centroid. Both $M_{eff\text{-}cen}$ and κ of uncracked and fully cracked sections can be found from a simple section analysis, thus giving the respective EI_{eq}.

Mechanical behavior of constituents

Concrete—Hognestad's parabolic stress-strain curve (Eq. (8))[8] is assumed for concrete in compression on loading, where σ_c is the stress at strain ε; f'_c is the cylinder strength; and ε_c and ε_{cu} are the strains at the maximum stress and the ultimate strain, respectively. A linear-elastic behavior is assumed for concrete in tension with the same modulus as the initial modulus in compression (E_{c0} in Eq. (9)).

Elastic unloading with modulus E_{c0} is assumed for concrete in both tension and compression. For the loading curve up to the maximum stress

$$\sigma_c = f_c' \{2(\varepsilon/\varepsilon_c) - (\varepsilon/\varepsilon_c)^2\} \Rightarrow \text{for } \varepsilon \le \varepsilon_c \quad (8)$$

$$E_{c0} = \frac{2f_c'}{\varepsilon_c} \quad (9)$$

Steel—Steel is assumed to be linear-elastic with modulus E_s up to yield at stress f_y, after which it is perfectly plastic on loading. It will be assumed to unload elastically with modulus E_s from any stress state.

FRP plate—The FRP plate is assumed to be linear-elastic with modulus E_p and herein there is no need to consider the strength of the FRP. Failure occurs either by plate debonding (when the plate can be assumed to be elastic) or by tensile fracture of the FRP (when the debonding analysis is irrelevant).[9] The adhesive will be assumed to be linear-elastic, although its properties have little effect on the strain energy calculation.

Effective moment on reinforced concrete section

To estimate the uncracked and fully cracked effective stiffness (Eq. (7)), the effective moments about the relevant centroidal axes ($M_{eff\text{-}cen}$) should be known. The value of $M_{eff\text{-}cen}$ can be calculated from Eq. (4) but the relevant centroidal axis depth α needs to be known. Centroidal axes are determined by defining equivalent transformed sections, but the varying concrete stiffness over the compressive zone and the reduction in the secant modules of steel after yielding should also be taken into account.

Equivalent section dimensions

The secant modulus of the steel is used to define the transformed sections, but a unique modulus for compressive concrete cannot be used because the concrete is assumed to be nonlinear. The varying modulus, however, can be included by defining equivalent widths (as is done when analyzing a beam made from two dissimilar materials when a modular ratio is used). Assuming the σ-ε relationship (Eq. (8)) and a linear strain variation across the RC section, the equivalent width at depth z from the beam top is

$$b(z) = b\left\{1 - \frac{\varepsilon_2}{2\varepsilon_c}\left(1 - \frac{z}{x}\right)\right\} \quad (10)$$

where b is the width of the beam section, ε_2 is the strain at the top of the beam, and x is the neutral axis depth. The transformed section can then be analyzed using the initial modulus for concrete E_{c0}.

These procedures allow the locations of the centroidal axes of the uncracked and fully cracked sections, and hence the respective effective moments, to be calculated from Eq. (4). With the already known curvatures, it is possible to determine the corresponding equivalent elastic stiffness from Eq. (7).

Effective equivalent elastic stiffness for partially cracked section

The effective equivalent elastic stiffness for the partially cracked section ($EI_{eq\text{-}eff}$) is then interpolated between the uncracked ($EI_{eq\text{-}un}$) and fully cracked ($EI_{eq\text{-}fc}$) stiffnesses, using the interpolation coefficient (K_p) taken from Eq. (6). When the section is uncracked ($M_{app\text{-}mid} < M_{cr\text{-}mid}$), K_p is set to 1; and when fully cracked ($M_{app\text{-}mid} > M_{y\text{-}mid}$), it is set to 0

$$EI_{eq\text{-}eff} = K_p EI_{eq\text{-}un} + (1 - K_p) EI_{eq\text{-}fc} \quad (11)$$

Curvature of section

The effective equivalent elastic stiffness ($EI_{eq\text{-}eff}$) calculated from Eq. (11) is relative to the effective centroid of the section.[10] Hence, if the effective moment about this axis ($M_{eff\text{-}cen}$) is known, the curvature κ of the section can be calculated from

$$\kappa = \frac{M_{eff\text{-}cen}}{EI_{eq\text{-}eff}} \quad (12)$$

The location of the effective centroid must be known to determine $M_{eff\text{-}cen}$ from Eq. (4). Sakai and Kakuta[11] presented a Branson-type expression for the effective centroidal axis depth α_{eff} of an RC beam section subjected to combined bending and axial force; α_{eff} is interpolated between the centroids of the corresponding uncracked and fully cracked sections (α_{un} and α_{fc}, respectively). The present model uses Sakai and Kakuta's approach to define the effective centroid α_{eff} of a strengthened section

$$\alpha_{eff} = C_p \alpha_{un} + (1 - C_p) \alpha_{fc} \quad (13)$$

where α_{un} and α_{fc} are known from the relevant section analysis. The interpolation coefficient C_p is defined in the same way as K_p in Eq. (6) but, following the discussions in References 7 and 8, the exponent is taken as 3.5 instead 4, which gives a better fit to the test data. The value of C_p in Eq. (14) is taken as 1 and 0 for uncracked and fully cracked sections, respectively

$$C_p = \left(\frac{M_{cr\text{-}mid}}{M_{app\text{-}mid}}\right)^{3.5}\left\{1 - \left(\frac{M_{app\text{-}mid} - M_{cr\text{-}mid}}{M_{y\text{-}mid} - M_{cr\text{-}mid}}\right)^{3.5}\right\} \quad (14)$$

Effective neutral axis depth

The neutral axis depths for the uncracked and fully cracked sections are known, but an expression for that of the effective section is still required. In the present model, the position of the effective neutral axis x_{eff} is interpolated between those of the corresponding uncracked (x_{un}) and fully cracked (x_{fc}) sections using the same coefficient used for the centroidal axis (C_p in Eq. (14)). Thus

$$x_{eff} = C_p x_{un} + (1 - C_p) x_{fc} \quad (15)$$

Now that the location of the neutral axis and the curvature can be calculated, it is possible to determine the strain distribution across the section, which can be used to determine the stress in the FRP plate.

Calculation of force in FRP plate

Everything that has been described so far can be calculated, provided the force in the FRP plate (F_p) is known. This must be chosen in such a way that the compatibility condition is satisfied. Two versions of this condition exist. If the FRP plate is still bonded to the beam, then strain compatibility must be satisfied locally between the FRP plate and the strain

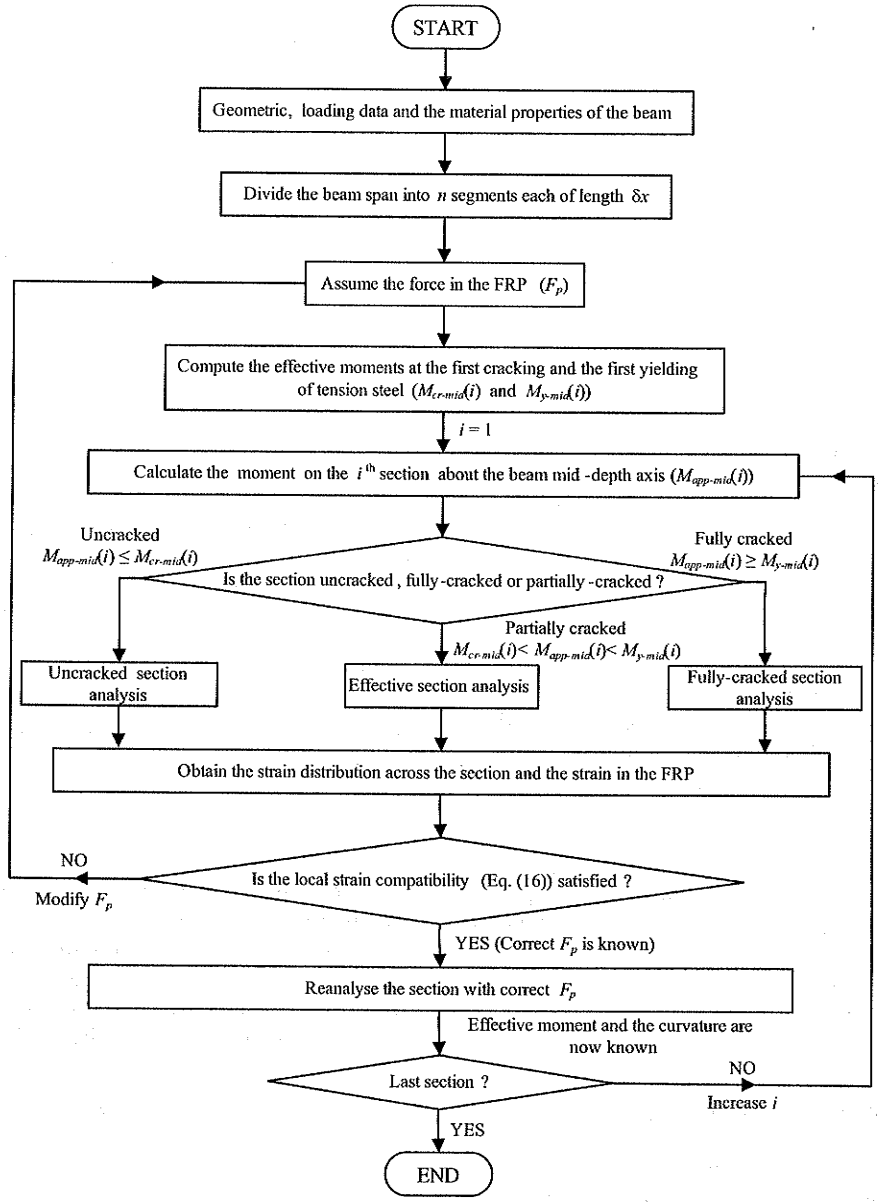

Fig. 3—Step-by-step procedure to calculate response in bonded region.

in the tension fiber of the concrete. When the FRP plate has debonded, then the weaker condition has to be satisfied in which the extension of the plate in the debonded region is the same as the extension of the tension fiber in the concrete.

The equations have been set up in a computer program, using an assumed value of F_p and a solution sought using the built-in solving routines, which find a solution for a set of nonlinear equations by a least-square method.

Local strain compatibility for a section with a bonded FRP plate—Strain in the FRP plate can be calculated from the local strain compatibility across the section. When the correct solution has been found, it will be the same as that directly derived from the assumed F_p

$$\frac{F_p}{E_p A_p} = \kappa \times (h + t_a + t_p/2 - x_{eff}) \qquad (16)$$

where E_p and A_p are the modulus and the cross-sectional area of the FRP plate; t_a, t_p, and h are as defined in Eq. (4). The values κ and x_{eff} are found from Eq. (12) and (15), respectively.

Global compatibility for sections with a debonded FRP plate—Over the debonded region, the change in length of the bottom fiber of the concrete beam should be compatible with that of the FRP plate

$$\int_{length\ l_d} \kappa(h + t_a + t_p/2 - x_{eff})dx = \frac{F_p}{E_p A_p} l_d \qquad (17)$$

where l_d is the length of the debonded zone.

Actual effective moment and curvature

Once the correct value of F_p is known, all the other parameters can be determined. Flowcharts (Fig. 3 and 4) for the complete process to determine $M_{eff\text{-}cen}$ and κ of RC sections with external FRP plates which may be bonded or partially debonded can also be downloaded from an associated Web site.[12]

VALIDATION

The model can predict M-κ relations of RC beams in the presence of a net axial force, and these can be compared with

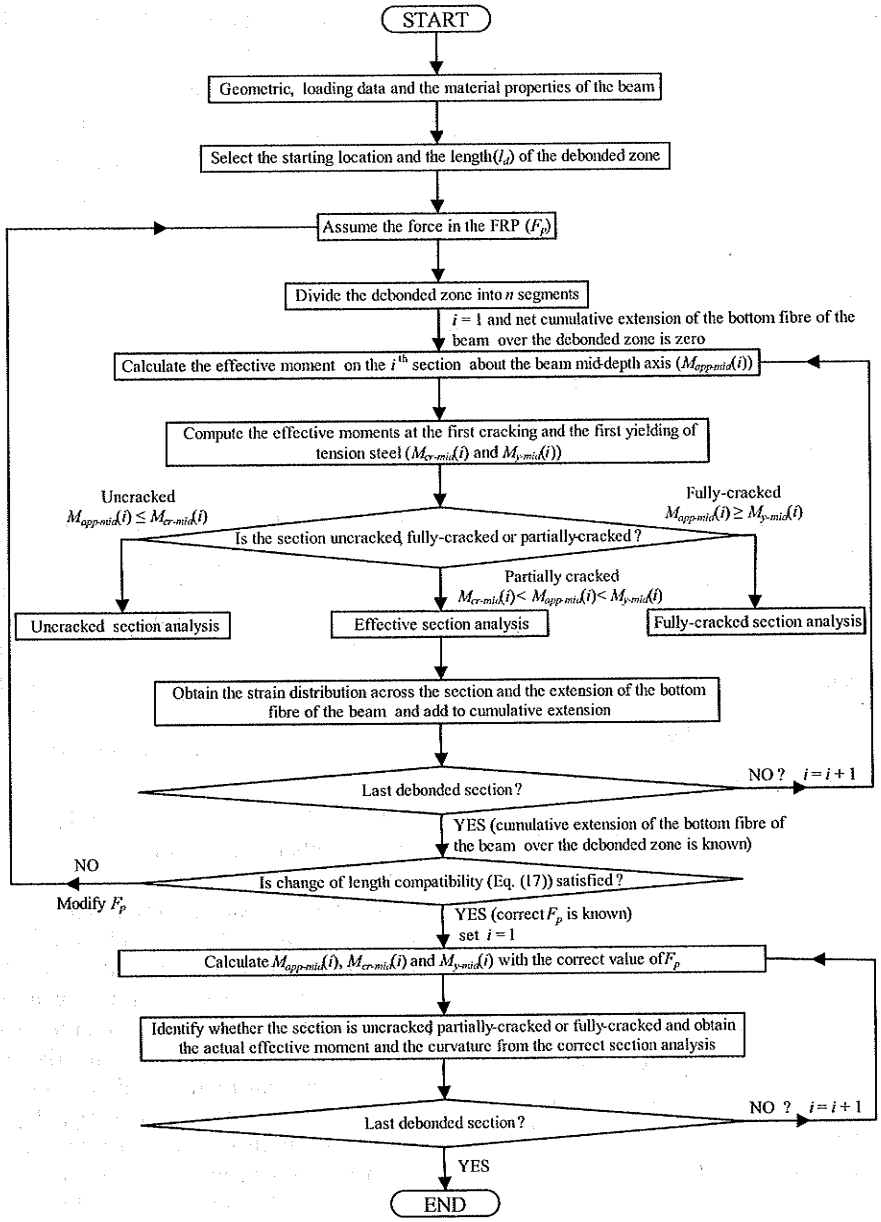

Fig. 4—Step-by-step procedure to calculate response in partly-debonded region.

published test data. The axial force can be either externally applied or exists due to unbalanced stress resultants acting on the RC section as in the case of RC beams with external FRP plates, in which case the net axial force is unknown at the beginning of the analysis. Comparisons between the test data and the present model can be made for some of the test specimens found from the literature under both of these categories. Due to space constraints, only a few such comparisons will be shown herein, but they cover test specimens with a large variety of material and geometric properties. The model can also be used to determine strain and deflection profiles of strengthened RC beams, and some comparisons of these parameters with relevant test data are also presented.

Material and geometric properties for analyses

For all the comparisons shown in the following, the yield stress and the elastic modulus of deformed steel bars are taken as 530 N/mm^2 (77 ksi) and 200 kN/mm^2 (29,000 ksi), respectively. This value for the yield strength has been taken because it represents a typical value for the actual strength of reinforcing bar. Even when values are quoted, in most papers, they are given as nominal or characteristic values supplied by the manufacturer and are not the result of direct tests. When test results are reported, they are in the range 500 to 550 N/mm^2 (72 to 80 ksi).[13,14] For concrete, strain at the maximum compressive stress (ε_c) is taken as 0.0022,[7] which is a reasonable value for the sort of normal strength concretes likely to have been used in beams needing repair and in the beams with which comparisons are made in this paper. (Note that this is not the strain at failure). The flexural tensile strength f_r is derived from Eq. (18),[6] although as with the tensile strength of all brittle materials, it shows high scatter. Published data is used for the other material properties when available; if not, the following values are used in the comparisons. When the cube strength f_{cu} is reported, the cylinder strength f_c' of concrete is taken as 80% of f_{cu}. If the characteristic strength f_{ck} of concrete is recorded, then the mean strength f_{cm} is derived from Eq. (19)

Table 1—Identification and material properties for fiber-reinforced polymer-strengthened test specimens[13-17]

Beam specimen	l_{span}, mm	l_{shear}, mm	l_{FRP}, mm	b, mm	h, mm	d, mm	d_c, mm	t_p, mm	t_a, mm	A_p, mm	A_{st}, mm	A_{sc}, mm	f_c', N/mm^2	E_p, kN/mm^2
A3.1[13]	4800	1800	4700	140	300	263	37.0	1.20	2*	96.0	402.0	402	24.0	152
A4[14]	2000	700	1700	200	200	163	37.0	1.30	2*	195.0	308.0	308	31.0	167
A6[14]	2000	700	1700	200	200	163	37.0	1.30	2*	390.0	308.0	308	31.0	167
A[15]	1100	400	1040	130	200	165*	35.0*	1.30	2*	120.0	101.0	101	37.0	120
CB4-2S[16]	4576	1830	4270	230	380	330	29.5	1.40	3	212.8	981.8	127	40.0	138
CB5-3S[16]	4576	1830	4270	230	380	330	29.5	1.40	3	319.2	981.8	127	40.0	138
G2[17]	2742	914	2742	200	200	152	41.0*	0.45	2*	91.4	259.0	142	54.8	138
G5[17]	2742	914	2742	200	200	152	41.0*	0.45	2*	91.4	774.0	142	54.8	138

*Assumed.

Notes: 1 mm = 0.039 in.; 1 N/mm^2 = 0.145 ksi; and 1 kN/mm^2 = 145.0 ksi.

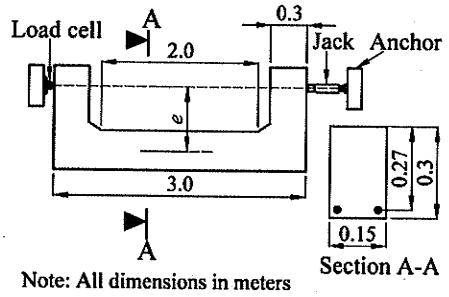

Fig. 5—Test specimen and loading method.[11] (Note: 1 m = 39.4 in.)

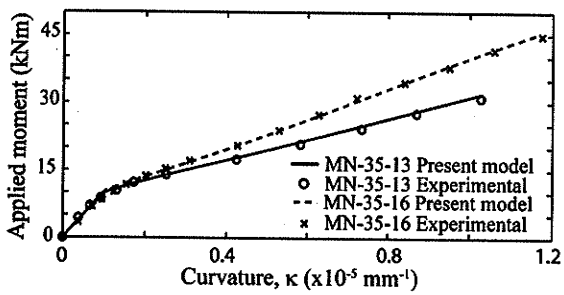

(a) **MN-35-13 and MN-35-16** [11]

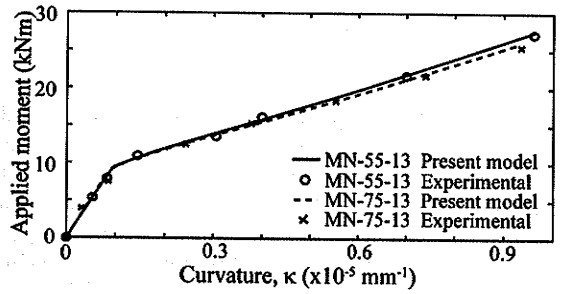

(b) **MN-55-13 and MN-75-13** [11]

Fig. 6—M-κ comparison. (Note: 1 kNm = 0.738 ft-kips; 10^{-5} mm^{-1} = 2.54 × 10^{-4} in.$^{-1}$)

$$f_r = 0.62\sqrt{f_c'} \text{ N/mm}^2 \quad (f_r = 7.5\sqrt{f_c'} \text{ psi}) \tag{18}$$

$$f_{cm} = f_{ck} + 8 \text{ N/mm}^2 \quad (f_{cm} = f_{ck}\ 1160 \text{ psi}) \tag{19}$$

When it is not reported, cover to the shear links is taken as 25 mm (1 in.) and the adhesive thickness as 2 mm (0.08 in.).

Table 2—Mechanical properties of materials[11]

Beam	Eccentricity e, mm	Steel ρ, %	f_c', N/mm^2
MN-35-13	350	0.596	31.0
MN-35-16	350	0.932	30.7
MN-55-13	550	0.596	30.7
MN-75-13	750	0.596	31.7

Notes: 1 mm = 0.039 in. and 1 N/mm^2 = 0.145 ksi.

Self-weight of the test specimens is not included in the analysis. All the other relevant material and geometric properties are given in Table 1.

Reinforced concrete beams subjected to combined bending and axial force—Sakai and Kakuta[11] reported M-κ relations of eight RC beam specimens subjected to combined bending and axial force. The specimens were of the form shown in Fig. 5, and the properties of four test specimens are described in Table 2. Figure 6 shows comparisons between the test data and the present model, which shows good agreement. The predicted cracking moment M_{cr} depends on the assumed tensile strength of the concrete (f_r), which is difficult to determine precisely even when checking an existing beam experimentally, but a reasonable assumed value (such as Eq. (18)) can still be appropriate. Comparisons with their other tests gave similarly good results. The reported data relate to the elastic regime of the beam so comparisons of the post-yield behavior cannot be made. No other model is available that allows such detailed comparison for beams under combined bending and axial force; this is the fundamental justification for the present study.

Present model predictions for FRP-strengthened RC beams—Some of the reported test data on M-κ relations as well as strain and deflection profiles of FRP-strengthened RC beam specimens are compared with predictions of the present model and show good correlation. All the test specimens reported were tested as simply supported beams under four-point bending with two equal shear spans and the reported failure mode was concrete crushing in the compression zone. The experimental data presented herein has been scaled from figures shown in the original references.[13-17] A large variety of material and geometric properties are covered, as described in Table 1.

Figure 7 shows M-κ comparisons for Beam A3.1 tested by Spadea et al.[15] It shows that the model can successfully predict behavior for all uncracked, partially cracked, and fully cracked regimes. The predicted M_{cr} and M_y are slightly

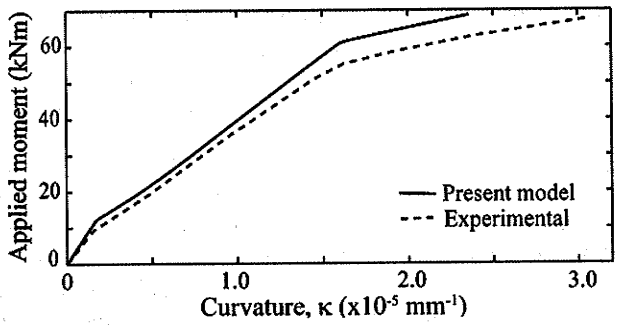

Fig. 7—M-κ comparison for Beam A3.1.[15] *(Note: 1 kNm = 0.738 ft-kips; 10^{-5} mm^{-1} = 2.54 × 10^{-4} $in.^{-1}$)*

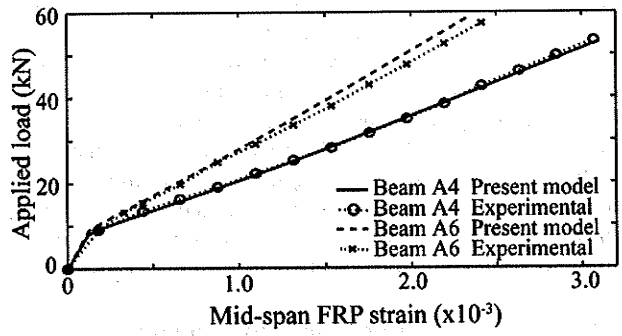

Fig. 8—FRP strain comparison.[13] *(Note: 1 kN = 0.225 kips.)*

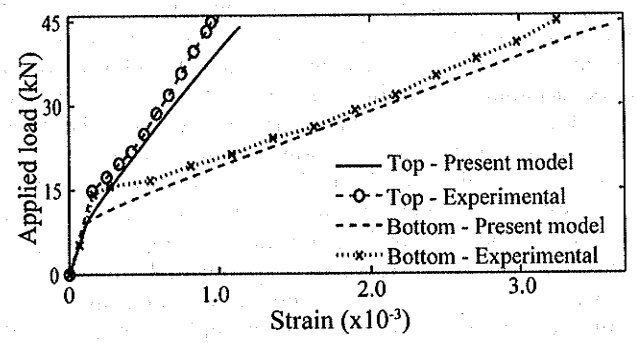

Fig. 9—Midspan top and bottom fiber strains of Beam A.[14] *(Note: 1 kN = 0.225 kips.)*

larger than those actually observed, which may be attributed to the overestimation of the concrete tensile strength or the steel yield strength. The small variations in the stiffness predictions may be attributed a slight overestimation of the material stiffness. Comparisons with the midspan FRP plate strains reported by Arduini et al.[13] are shown in Fig. 8. The data covers only the preyield regime, which shows good correlation. Figure 9 shows the comparisons for the reported top and bottom fiber strain data for Beam A tested by Li et al.[14] Satisfactory agreement can be seen; the model correctly predicts strain profile across a section, validating both the present effective stiffness concept and effective neutral axis expression (Eq. (15)). Comparisons with the FRP plate strain data at three different span locations of Beam CB4-2S tested by Alagusundaramoorthy et al.[16] are shown in Fig. 10. Good correlations can be observed in all cases. This shows that, not only does the model correctly predict the curvatures, but it also correctly predicts the neutral axes, from which it can be assumed that the strain profiles will be correct.

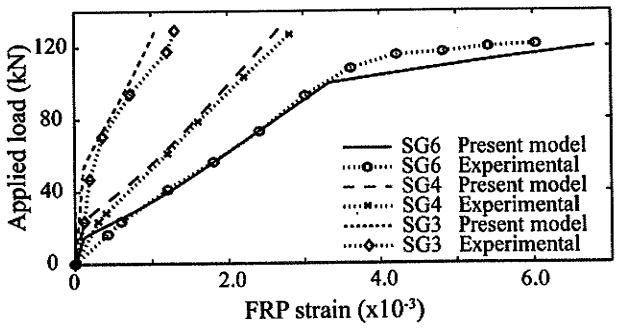

Fig. 10—FRP strain comparisons along span of Beam CB4-2S.[16] *(Note: 1 kN = 0.225 kips.)*

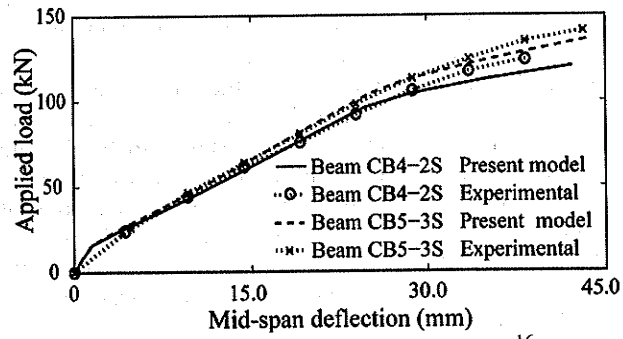

(a) **Beams CB4-2S and CB5-3S** [16]

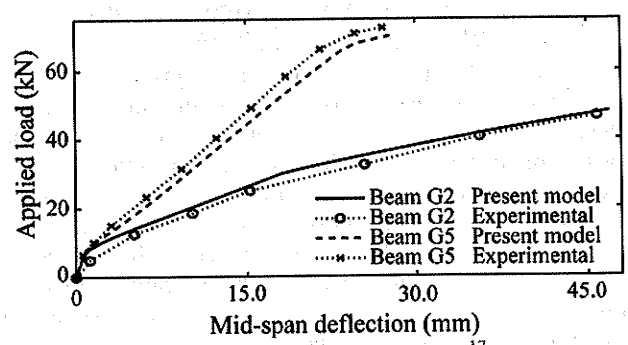

(b) **Beams G2 and G5** [17]

Fig. 11—Midspan deflection comparisons. (Note: 1 kN = 0.225 kips; 1 mm = 0.039 in.)

Deflections are not calculated directly but must be found by integration of curvatures; comparisons between such midspan deflection predictions and the relevant test data for a few beams reported by Alagusundaramoorthy et al.[16] and Ross et al.[17] are shown in Fig. 11. The predictions at lower loads are smaller than those observed, which implies that the material stiffness used in the analysis has been slightly overestimated, but the comparisons show a satisfactory agreement at higher loads for a model relating to reinforced concrete. This satisfaction of deflection estimations confirms the accuracy of the predicted curvatures.

Confirmation of model

The previous comparisons show that the present model accurately predicts *M*-κ relations and strain profiles of strengthened RC beam sections, but at lower applied moments, the present model is slightly stiffer than the experiments. Possible errors involved with measuring smaller quantities, together with the inaccuracies in the material properties used in the analysis (especially the modulus and the tensile

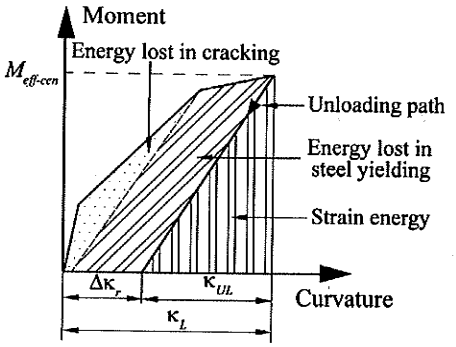

Fig. 12—Energy in flexure.

strength of concrete that have been calculated using Eq. (8) and (18), respectively, from the quoted values of the compressive strength) may be the cause of this discrepancy. Slight discrepancies are also observed near the failure load, which may be due to possible cracking in compressive concrete and onset of FRP plate debonding failures just prior to the ultimate failure that are not included in the present analysis. These minor inaccuracies, however, are to be expected in models of reinforced concrete, and it can be concluded that the present model predicts M-κ relations on loading with sufficient accuracy that can be used as the basis for strain energy determinations.

FLEXURAL STRAIN ENERGY STORED IN STRENGTHENED BEAM

The overall objective of the model is not just to predict the curvatures, but to accurately calculate the strain energy. When a beam bends, energy is put into the beam by the loads, some of which is dissipated in the concrete, either in flexural-tension cracking or material nonlinearity and some by yielding of the steel reinforcement, whereas the rest is stored as strain energy that can be recovered when the beam is completely unloaded, as shown schematically in Fig. 12. This recoverable energy is known if the corresponding unloading M-κ relations are known.

Unloading M-κ relations

The unloading M-κ relations of a strengthened section can be determined in the same way as the loading curves, but with the unloading properties of the constituents, and for actions applied along the opposite directions to those upon loading. It is assumed that all the constituents are linear-elastic upon unloading, so the corresponding M-κ relations are linear irrespective of the moment from which the unloading takes place. Thus, the flexural strain energy (SE) available in a beam segment of unit length at a given effective moment $M_{eff\text{-}cen}$ is shown in Fig. 12 and calculated from

$$SE = \frac{1}{2} M_{eff\text{-}cen} \kappa_{UL} \tag{20}$$

where $M_{eff\text{-}cen}$ is already known from the loading analysis, but the corresponding change in curvature upon complete unloading (κ_{UL}) is unknown.

The values obtained from Eq. (20) are then integrated along the beam span and added to the strain energy in the FRP and the axial effects of the concrete. Full details are given elsewhere. [2]

Change in curvature upon complete unloading

As shown in Fig. 12, only the change in curvature upon complete unloading (κ_{UL}) from $M_{eff\text{-}cen}$ is required for the strain energy determination. The value of κ_{UL} can be determined from section analysis for the actions of equal magnitude but opposite sense to those applied upon loading. Therefore, in the present model, a strengthened section is analyzed for an axial force (F_p) and moment ($M_{eff\text{-}cen}$) both acting along the opposite directions to those upon loading.

It is assumed that the steel and concrete are both linearly elastic, with the extent of cracking as found from the loading analysis. This matches reasonably with test data,[18] which shows that there is some residual strain when the structure has been completely unloaded.

This unloading section analysis is applicable with uncracked and fully cracked sections, for which the tensile contribution of concrete is exactly known. The RC section is taken as uncracked for applied moments ($M_{app\text{-}mid}$) smaller than that causing first cracking ($M_{cr\text{-}mid}$), and the section is fully cracked when $M_{app\text{-}mid}$ is greater than that causing first yielding of tension steel ($M_{y\text{-}mid}$). Therefore, the change in curvature upon complete unloading at applied moments smaller than $M_{cr\text{-}mid}$ and greater than $M_{y\text{-}mid}$ can be found. The situation is more complex when the section is partially cracked.

Change in curvature of partially cracked sections

The present loading model interpolates the properties of a partially cracked section (that is, when $M_{cr\text{-}mid} < M_{app\text{-}mid} < M_{y\text{-}mid}$) between those of the corresponding uncracked and fully cracked sections. This interpolation is based on the present-extent-of-cracking concept (Eq. (6)) and has proven to be accurate. A similar concept will be used for the unloading analysis of partially cracked sections. There is little experimental evidence, however, to confirm whether expressions similar to those for the effective equivalent elastic stiffness (Eq. (11)) and the effective centroid (Eq. (13)) used in the present loading analysis are applicable upon unloading. Morais[18] reported experimental findings of unloading deflection data for concrete beams internally reinforced with either steel or aramid fiber-reinforced polymer rods. The focus was on the unloading behavior from the vicinity of the ultimate failure; approximately linear unloading paths were experienced. These data, however, are insufficient to study the unloading behavior over the entire load range. To avoid having to define effective values for the stiffness and the centroidal location, a slightly modified form of the interpolation used in the loading analysis is employed to determine the change in curvature upon complete unloading of a partially cracked section.

Curvature upon loading and the corresponding change in curvature upon complete unloading of the section at $M_{cr\text{-}mid}$ and $M_{y\text{-}mid}$ can be calculated from the relevant uncracked and fully cracked section analysis, respectively. The residual curvatures are then determined ($\Delta\kappa_{r\text{-}cr}$ from the state at first cracking and $\Delta\kappa_{r\text{-}y}$ from the first yielding state). The corresponding residual curvature of a partially cracked section ($\Delta\kappa_r$) is then interpolated between these values by

$$\Delta\kappa_r = K_p \Delta\kappa_{r\text{-}cr} + (1 - K_p)\Delta\kappa_{r\text{-}y} \tag{21}$$

where the interpolation coefficient is the extent-of-cracking parameter that is already known from the loading analysis (K_p in Eq. (6)). Because the curvature upon loading (κ_L) is

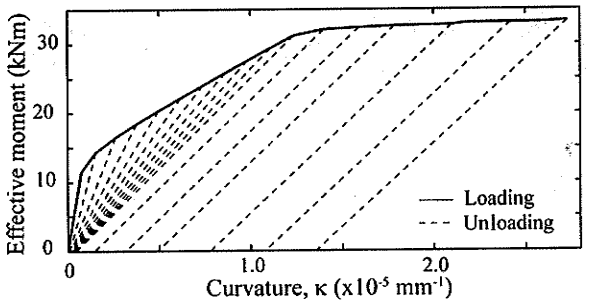

Fig. 13—Loading and unloading curvatures. (Note: 1 kNm = 0.738 ft-kips; and 10^{-5} m^{-1} = 2.54 × 10^{-4} $in.^{-1}$)

known (κ in Eq. (12)), the unloading curvature is then calculated from

$$\kappa_{UL} = \kappa_L - \Delta\kappa_r \tag{22}$$

The present model can thus be used to predict both the loading and unloading M-κ relations of FRP strengthened RC beams. A typical result is shown in Fig. 13.

Complex stress distributions in vicinity of neutral axis

At any given applied moment, the section's neutral axes depths upon loading and complete unloading (x_L and x_{UL}, respectively) are not identical. Depending on the relative locations of x_L and x_{UL}, some concrete that cracked in tension upon loading may now be subjected to compressive stresses upon unloading or vice-versa. In both cases, the actual unloading stress distributions over these concrete zones would differ from those used in the present analysis. These complex stress zones are located in the vicinity of the neutral axis, so the stresses will be small and will make little contribution to the strain energy of the beam. Thus, no attempt has been made to resolve this issue as it is thought to be a minor error by comparison with the natural variability of concrete.

CONCLUSIONS

A moment-curvature model has been presented for the strain energy determinations of RC beams with external FRP plates. The model is valid for the full range of applied moments of the strengthened beam and includes nonlinear stress-strain relationships of constituents and also the tension stiffening effects of cracked concrete.

It has been shown how the model can be extended into the inelastic regime and also how axial forces are taken into account. Comparisons with the available test data have demonstrated that the present model is accurate.

The model has then been used to calculate the stored strain energy on the assumption that the beam would unload elastically from any loaded state. Tension stiffening effects of cracked concrete are included in the analysis both on loading and unloading.

This model can now be applied to the study of plate debonding. The results of that study are the subject of a separate publication.[2]

The model should also be valid for combined bending and axial force in general and so should be applicable to prestressed concrete, but it has not been calibrated for the much higher levels of axial force present in such beams, which are rarely cracked to the extent envisaged herein.

ACKNOWLEDGMENTS

The first author was sponsored in this work by the Overseas Research Studentships (ORS) and the Cambridge Commonwealth Trust, and is appreciative of their financial assistance.

NOTATION

A_p = cross sectional area of FRP plate
A_{sc} = area of compression reinforcement
A_{st} = area of tension steel reinforcement
b = width of RC section
d = effective depth to tension steel
d_c = effective depth to compression steel
E_p = Young's modulus of FRP plate
f_c' = compressive strength of concrete
h = height of RC section
l_{FRP} = length of FRP plate
l_{shear} = shear span of beam specimen
l_{span} = effective span of beam specimen
t_a = thickness of adhesive layer
t_p = thickness of FRP plate

REFERENCES

1. Hutchinson, J. W., and Suo, Z., "Mixed Mode Cracking in Layered Materials," *Advances in Applied Mechanics*, J. W. Hutchinson and T. Y. Wu, eds., V. 29, 1992, pp. 63-191.

2. Achintha, P. M. M., and Burgoyne, C. J., "Fracture Mechanics of Plate Debonding," *Journal of Composites for Construction*, V. 12, No. 4, 2008, pp. 396-404.

3. Branson, D. E., "Design Procedures for Computing Deflections," ACI JOURNAL, *Proceedings* V. 65, No. 9, Sept. 1968, pp. 730-735.

4. Faruqi, M.; Wu, C. C.; and Benson, F., "Development of Deflection Equations Using Moment-Curvature Relationship for Reinforced Concrete Beams Strengthened with Fibre Reinforced Polymer (FRP) Plates," *Magazine of Concrete Research*, V. 55, No. 6, 2003, pp. 549-557.

5. El-Mihilmy, M. T., and Tedesco, J. W., "Defections of Concrete Beams Strengthened with Fiber-Reinforced Polymer (FRP) Plates," *ACI Structural Journal*, V. 97, No. 5, Sept.-Oct. 2000, pp. 679-688.

6. ACI Committee 318, "Building Code Requirements for Structural Concrete (ACI 318-08) and Commentary," American Concrete Institute, Farmington Hills, MI, 2008, 465 pp.

7. British Standards Institution, "Eurocode 2: Design of Concrete Structures," London, UK, 1992, pp. 251-252.

8. Hognestad, E.; Hanson, N. W.; and McHenry, D., "Concrete Stress Distribution in Ultimate Strength Design," ACI JOURNAL, *Proceedings* V. 52, No. 4, Apr. 1955, pp. 455-480.

9. Buyukozturk, O.; Gunes, O.; and Karaca, E., "Progress on Understanding Debonding Problems in Reinforced Concrete and Steel Members Strengthened using FRP Composites," *Construction and Building Materials*, V. 18, No. 1, 2004, pp. 9-19.

10. Teng, S., and Branson, D. E., "Initial and Time-Dependent Deformation of Progressively Cracking Nonprestressed and Partially Prestressed Concrete Beams," *ACI Structural Journal*, V. 90, No. 5, Sept.-Oct. 1993, pp. 480-488.

11. Sakai, K., and Kakuta, Y., "Moment-Curvature Relationships of Reinforced Concrete Members Subjected to Combined Bending and Axial Force," ACI JOURNAL, *Proceedings* V. 77, No. 3, Mar. 1980, pp. 189-194.

12. http://www-civ.eng.cam.ac.uk/cjb/frpdebond/.

13. Arduini, M.; Di Tommaso, A.; and Nanni, A., "Brittle Failure in FRP Plate and Sheet Bonded Beams," *ACI Structural Journal*, V. 94, No. 4, July-Aug. 1997, pp. 363-370.

14. Li, A.; Assih, J.; and Delmas, Y., "Shear Strengthening of RC Beams with Externally Bonded CFRP Sheets," *Journal of Structural Engineering*, V. 127, No. 4, 2001, pp. 374-380.

15. Spadea, G.; Bencardino, F.; and Swamy, R. N., "Structural Behaviour of Composite RC Beams with Externally Bonded CFRP," *Journal of Composites for Construction*, V. 2, No. 3, 1998, pp. 132-137.

16. Alagusundaramoorthy, P.; Harik, E.; and Choo, C. C., "Flexural Behaviour of RC Beams with Carbon Fibre Reinforced Polymer Sheets or Fabric," *Journal of Composites for Construction*, V. 7, No. 4, 2003, pp. 292-301.

17. Ross, C. A.; Jerome, D. M.; Tedesco, J. W.; and Hughes, M. L., "Strengthening of Reinforced Concrete Beams with Externally Bonded Composite Laminates," *ACI Structural Journal*, V. 96, No. 2, Mar.-Apr. 1999, pp. 212-220.

18. Morais, M. M., "Ductility of Beams Prestressed with FRP Tendons," PhD thesis, University of Cambridge, UK, 2005.